# The methyltransferase NSD3 promotes antiviral innate immunity via direct lysine methylation of IRF3

Chunmei Wang,[1,2] Qinlan Wang,[3] Xiaoqing Xu,[1] Bin Xie,[3] Yong Zhao,[4] Nan Li,[2] and Xuetao Cao[1,2,3]

[1]Department of Immunology and Center for Immunotherapy, Institute of Basic Medical Sciences, Peking Union Medical College, Chinese Academy of Medical Sciences, Beijing, China
[2]National Key Laboratory of Medical Immunology and Institute of Immunology, Second Military Medical University, Shanghai, China
[3]Institute of Immunology, Zhejiang University School of Medicine, Hangzhou, China
[4]Department of Genetics and Genomic Sciences, Icahn School of Medicine at Mount Sinai, New York, NY

**Lysine methylation is an important posttranslational modification, implicated in various biological pathological conditions. The transcription factor interferon regulatory factor 3 (IRF3) is essential for antiviral innate immunity, yet the mechanism for methylation control of IRF3 activation remains unclear. In this paper, we discovered monomethylation of IRF3 at K366 is critical for IRF3 transcription activity in antiviral innate immunity. By mass spectrometry analysis of IRF3–associated proteins, we identified nuclear receptor–binding SET domain 3 (NSD3) as the lysine methyltransferase that directly binds to the IRF3 C–terminal region through its PWWP1 domain and methylates IRF3 at K366 via its SET domain. Deficiency of NSD3 impairs the antiviral innate immune response in vivo. Mechanistically, NSD3 enhances the transcription activity of IRF3 dependent on K366 monomethylation, which maintains IRF3 phosphorylation by promoting IRF3 dissociation of protein phosphatase PP1cc and consequently promotes type I interferon production. Our study reveals a critical role of NSD3-mediated IRF3 methylation in enhancing antiviral innate immunity.**

## INTRODUCTION

Posttranslational modifications (PTMs) play essential roles in various biological and immunological processes via altering the structural, conformational, and physicochemical properties of proteins (Deribe et al., 2010; Liu et al., 2016). Although the mechanisms and functions of conventional PTMs such as phosphorylation and ubiquitination in cellular pathways have been extensively elucidated, less is known about the roles of unconventional PTMs such as methylation, acetylation, and SUMOylation in the context of innate immunity and antiviral responses (Mowen and David, 2014). Protein methylation is an important PTM occurring at lysine or arginine residues. Specifically, lysine methylation critically regulates cellular signaling and function, not only at the histone level by controlling DNA transcription and chromatin remodeling, but also at the nonhistone level by modifying the activity of numerous signaling molecules, cytoskeleton proteins, and transcription factors (TFs), leading to diversified biological effects (Biggar and Li, 2015; Gunawan et al., 2015; Hamamoto et al., 2015; Park et al., 2016). Several TFs, such as p53, STATs, and NF-κB, have been shown to be regulated by various protein lysine methyltransferases for modulation of transcriptional activity and downstream signaling events (Chuikov et al., 2004; Ea and Baltimore, 2009; Dasgupta et al., 2015). For instance, enhancer of zeste homologue 2 (EZH2)–mediated methyla-

tion of STAT3 potently regulates STAT3-driven transcription and tumorigenesis (Kim et al., 2013; Dasgupta et al., 2015). NF-κB is regulated by reversible lysine methylation of the RelA subunit catalyzed by several lysine methyltransferases (Ea and Baltimore, 2009; Lu et al., 2010; Levy et al., 2011). Although these studies indicate the potentially important roles of methylation in regulation of inflammation and tumorigenesis, it's urgent to elucidate whether and how methylation and specific lysine methyltransferases could regulate antiviral innate immune responses.

Interferon regulatory factor 3 (IRF3) is a key TF responsible for induction of type I IFNs and plays a critical role in host antiviral innate immunity (Sadler and Williams, 2008). Dysregulation of IRF3-dependent antiviral innate immunity is linked to many immunological disorders, such as infectious and inflammatory diseases. Thus, identification of the regulatory mechanisms of IRF3 function is critical for better understanding of host antiviral innate responses and also has significant biological importance and clinical implication in the control of infectious and inflammatory diseases. IRF3 is constitutively expressed and localizes to the cytoplasm under steady state; upon innate recognition of pathogens, IRF3 is phosphorylated by TBK1 and IKKε, leading to the formation of IRF3 homodimers and subsequent translocation to the nucleus, where it activates the transcription of genes encoding type I IFN (Fitzgerald et al., 2003; Takeuchi

and Akira, 2009). Conversely, multiple mechanisms have also evolved to down-regulate IRF3 function to avoid unwanted immune pathology, majorly via PTMs of IRF3 (Mowen and David, 2014; Liu et al., 2016). For example, IRF3 is deactivated through dephosphorylation by some phosphatase, such as PTEN (Li et al., 2016a), protein phosphatase 2A (Long et al., 2014), or MAPK phosphatase (Png and Zhang, 2015), or through ubiquitination and proteasomal degradation by peptidylprolyl cis-/trans-isomerase, NIMA–interacting 1 (Pin1; Saitoh et al., 2006), E3 ligases RBCC protein interacting with PKC1 (Zhang et al., 2008), and RTA-associated ubiquitin ligase (Yu and Hayward, 2010). In addition, other forms of unconventional PTMs such as SUMOylation (Maarifi et al., 2016), S-glutathionylation (Prinarakis et al., 2008), and acetylation (Suhara et al., 2002) have been implicated in fine tuning of IRF3 activity. However, the roles of methylation for regulation of IRF3 function in antiviral immunity and the cross talk between methylation and conventional PTMs in this process remain unclear.

The nuclear receptor–binding SET domain (NSD) protein lysine methyltransferase family is composed of three members: NSD1, NSD2/MMSET/WHSC1, and NSD3/WHSC1L1. All NSD members share the similar structure consisting of a catalytic SET domain responsible for the methyltransferase activity, four PHD domains (PHD1–4), and two proline–tryptophan–tryptophan–proline (PWWP1 and PWWP2) domains involved in protein–protein interactions (Vougiouklakis et al., 2015). NSD proteins are implicated in tumorigenesis, metabolism, and inflammation via the catalyzing methylation of both histones and nonhistones (Wang et al., 2007; Yang et al., 2012). For example, NSD1 triggers leukemogenesis via up-regulating expression of HOXA through methylation of histone H3K36 (Wang et al., 2007) and promotes inflammatory responses via methylating the RelA subunit of NF-κB (Lu et al., 2010), and NSD2 regulates TWIST1, Wnt, and NF-κB signaling to promote oncogenic programming (Toyokawa et al., 2011; Yang et al., 2012; Ezponda et al., 2013). NSD3 is involved in human carcinogenesis via targeting NEK7 and CCNG1 (Kang et al., 2013) and also interacts with bromodomain proteins to regulate the transcription of target genes (Rahman et al., 2011). However, the role of the NSD family in mediating the lysine methylation of the innate TFs and their relevance in antiviral innate immunity remains unknown.

Here, we report a previously undescribed mechanism of regulating IRF3 transcription activity through lysine methylation catalyzed by NSD3 upon viral infection, providing a new mechanistic insight into methylation control of antiviral innate responses.

## RESULTS
### Monomethylation of IRF3 at K366 is critical for IRF3 transcription activity in antiviral innate immunity
Methylation is an important PTM essential for various cellular processes (Mowen and David, 2014). IRF3 is the key TF that activates the expression of type I IFNs, which are critical for innate antiviral responses, so we wondered whether methylation might be involved in regulation of IRF3 activity. We first detected the methylation status of IRF3 in TAP-IRF3 RAW264.7 cells (RAW264.7 cells with stable overexpression of TAP-tagged IRF3) in antiviral immune responses. The level of mono-/dimethylation at lysine was obviously enhanced by infection with HSV or vesicular stomatitis virus (VSV) and modestly enhanced by bacterial LPS stimulation in TAP-IRF3 RAW264.7 cells (Fig. 1 A). The level of mono-/dimethylation at lysine was also enhanced by VSV infection in primary peritoneal macrophages (PMs; Fig. 1 B).

We then performed mass spectrometry (MS) analysis in both untreated and VSV-infected TAP-IRF3 RAW264.7 cells to identify potential methylated lysine residues of IRF3. Three monomethylated lysine residues including K308, K366, and K381 were identified (Fig. 1 C). Although K308 and K381 methylation were present with or without VSV infection, K366 methylation could be only detected after VSV infection (Table S1). To further investigate whether these methylation sites of IRF3 could affect IRF3 transcriptional activity, we constructed methylation-defective IRF3 mutants with substitution at each lysine residue with alanine (K308A, K366A, and K381A) or arginine (K308R, K366R, and K381R), and double mutants with alanine or arginine substitution at both K366 and K381 (K366/K381A and K366/K381R), and methylation-mimicking mutant with phenylalanine substitution at K366 residue (K366F). Methylation-defective substitution at both K366 and K381, especially K366 (K366A and K366R), significantly abolished IRF3-driven *Ifnb* activation, but those at K308 had no such effect. The double mutants K366/K381A and K366/K381R showed greater inhibitory activity than single mutants. In contrast, methylation-mimicking substitution K366F significantly promoted IRF3-driven *Ifnb* activation (Fig. 1 D). In addition, a mass shift of 14 D was observed in VSV-infected cells for the IRF3 peptide VVPTCLK, which is consistent with monomethylation at the lysine K366 residue (Fig. 1 E). These findings suggest that monomethylation at the K366 site may be most likely responsible for the regulation of IRF3 transcription activity.

We then raised polyclonal antibodies against IRF3 peptides containing K366me1 and confirmed its specificity by showing its binding to the methylated peptide, but not to the corresponding unmodified peptide (Fig. S1 A). The level of monomethylation of IRF3 at K366 was significantly induced in TAP-IRF3 RAW264.7 cells by HSV, VSV, or influenza A virus infection, but not by TLR ligand stimulation (LPS, CpG ODN, or PolyI:C; Fig. 1 F). The similar results were observed in some kinds of cancer cells overexpressing NSD3 in response to VSV infection (Fig. S1 B). Thus, K366 monomethylation of IRF3 is selectively induced by viral infection. Moreover, overexpression of IRF3(K366A) in IRF3-deficient PMs and MEF
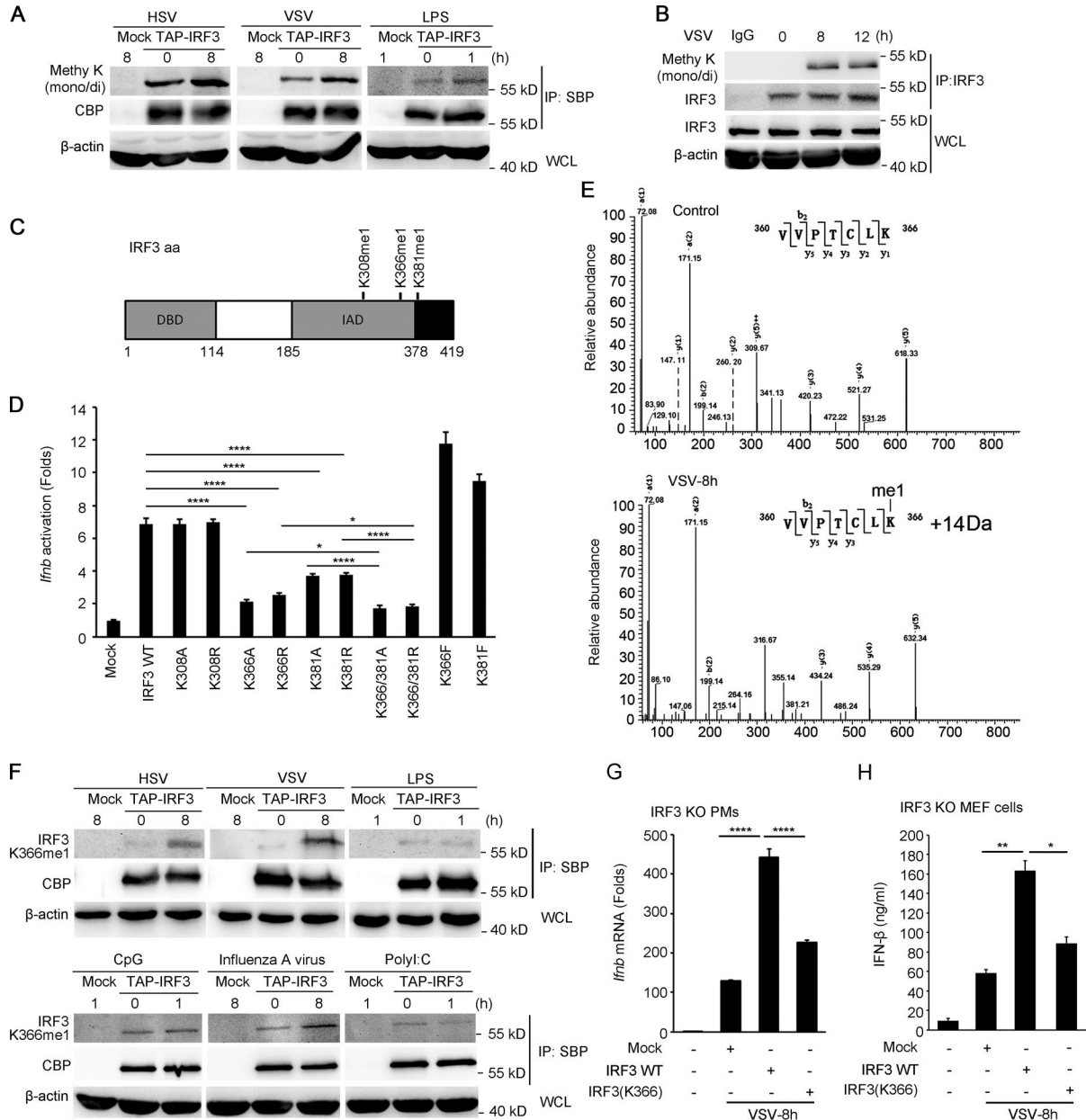
Figure 1. **K366 monomethylation of IRF3 in VSV-infected macrophages.** (A) Immunoblot analysis of mono-/dimethylation of IRF3 from TAP-IRF3 RAW264.7 cells infected with HSV (10 multiplicity of infection [MOI]) or VSV (1 MOI) or stimulated with LPS (100 ng/ml) for the indicated times. Cell lysates were immunoprecipitated with streptavidin-binding protein antibody–conjugated magnetic beads and then subjected to immunoblot analysis with anti-mono-/dimethylated antibody against TAP-tag IRF3. (B) Endogenous IRF3 immunoprecipitated with IRF3 antibody from PMs infected with VSV (1 MOI) for the indicated times was immunoblotted with the indicated antibodies. (C) Illustration of methylated lysine residues of IRF3 identified by MS assay. DBD, DNA-binding domain; IAD, interaction domain of IRF3. (D) Ifnb activation in HEK293T cells transfected with WT IRF3 or IRF3 mutants was analyzed by luciferase reporter assay. (E) The tryptic peptide IRF3 (360–366, VVPTCLK), consistent with a 14-D mass modification of K366, was identified in VSV-infected TAP-IRF3 RAW264.7 cells by MS analysis. Images are representative of two independent experiments. (F) IRF3 immunoprecipitated from virus-infected or TLR-stimulated TAP-IRF3 RAW264.7 cells was immunoblotted with the indicated antibodies. (G) PMs from IRF3-deficient mice were transfected with WT IRF3 or IRF3 mutants by nuclear transfection for 24 h and then infected with VSV (1 MOI) for 8 h. The level of mRNA of Ifnb was measured by Q-PCR. (H) MEF cells from IRF3-deficient mice were transfected with WT IRF3 or IRF3 mutants by FuGENE HD transfection reagent for 24 h and then infected with VSV (1 MOI) for 8 h. The production of IFN-β was measured by ELISA. Mock, empty control vector. (A, B, and F) Immunoblots are representative of three independent experiments. (D) Data are mean ± SEM and representative of three independent experiments (one-way ANOVA; n = 4–6 per group). (G and H) Data are mean ± SEM and representative of three independent experiments (unpaired, two-tailed Student's t test). *, P < 0.05; **, P < 0.01; ****, P < 0.0001. WCL, whole cell lysate.

cells significantly abrogated IRF3-dependent *Ifnb* activation and IFN-β production upon VSV infection (Fig. 1, G and H).

Collectively, these data indicate that viral infection induces monomethylation of IRF3 at K366, which is responsible for promoting IRF3 activation and IFN-β production.

## Lysine methyltransferase NSD3 directly binds to IRF3 and methylates IRF3

We then performed MS analysis to identify the potential protein or proteins mediating the monomethylation of K366 of IRF3. Two lysine-associated methyltransferases, NSD3 (with a higher score of 346; protein matches, 45) and Kmt2d (with a lower score of 18; protein matches, 2) were identified. A co-immunoprecipitation (IP) assay showed that FLAG-tagged IRF3 interacted with Myc-tagged NSD3 reciprocally in HEK293T cells (Fig. 2 A) and that the endogenously activated IRF3 bound to NSD3, but not Kmt2b in VSV-infected macrophages (Fig. 2 B and Fig. S2 A). We next sought to determine whether NSD3 could directly induce the K366 methylation of IRF3. K366 methylation of IRF3 was detected only when NSD3 was coexpressed in VSV-infected HEK293T cells (Fig. 2 C) and was completely blocked in VSV-infected macrophages derived from NSD3-deficient mice (Fig. 2 D). The decrease of IRF3 K366 methylation could be rescued by reintroducing NSD3 into NSD3-deficient MEF cells (Fig. 2 E), suggesting that methyltransferase NSD3 is required for K366 methylation of IRF3. Furthermore, in vitro methylation kinase assay showed that purified NSD3(SET) protein containing only the catalytic SET domain of NSD3 directly methylated the immunoprecipitated IRF3 (Fig. 2 F) as well as purified IRF3 protein (Fig. 2 G) at K366 in a dose-dependent manner. However, K366A-mutated IRF3 could not be methylated by NSD3(SET) (Fig. 2 E). Collectively, these results show that NSD3 directly methylates IRF3 at K366 upon viral infection.

To map the NSD3 domains required for the interaction with IRF3, we constructed five different Myc-tagged NSD3 truncations, respectively lacking PWWP1 (ΔPWWP1), PWWP1+PHD1–3 (ΔPWWP1+PHD1–3), PWWP2+SET+PHD4 (ΔPWWP2+SET+PHD4), SET+PHD4 domain (ΔSET+PHD4), or PHD4 domain (ΔPHD4; Fig. S2 B). Among the truncations, only those containing PWWP1 domain (ΔPWWP2+SET+PHD4, ΔSET+PHD4, and ΔPHD4) were able to interact with IRF3, whereas those lacking PWWP1 domain (ΔPWWP1 and ΔPWWP1+PHD1–3) could not (Fig. S2, C and D). Thus, PWWP1 domain is responsible for NSD3 interaction with IRF3. We further mapped the regions of IRF3 responsible for this interaction. IRF3 truncation containing the C-terminal region at 114–419 aa was able to interact with NSD3, whereas IRF3 truncation containing the N-terminal DNA-binding domain at 1–114 aa lost the ability (Fig. S2, E and F). These data demonstrated that NSD3 may interact with IRF3 C-terminal region through its PWWP1 domain.

## Deficiency of NSD3 impairs antiviral innate immune response in vivo

NSD3 has been shown to be involved in various cellular events such as carcinogenesis and metabolism. However, the role of NSD3 in innate immunity remains unknown. According to GEO profiling data, NSD3 exhibits an inducible expression upon infection with HIV (GEO accession no. GDS4225; Manel et al., 2010) and respiratory syncytial virus (GEO accession no. GDS2023; Huang et al., 2008). Consistently, NSD3 was significantly up-regulated in PMs by VSV infection (Fig. S3 A), which was dependent on IRF3 but not NF-κB signaling (Fig. S3, B and C), indicating the possible positive feedback role of NSD3 in regulating IFN/IRF3-triggered antiviral immunity. NSD3 deficiency (Fig. S3 D) didn't affect the differentiation (Fig. S3 E) or cell viability (Fig. S3 F) of macrophages. Compared with PMs from littermate control mice, NSD3-deficient PMs expressed significantly lower levels of IFN-β upon VSV infection (Fig. 3, A and B), which was reversed by NSD3 reintroduction (Fig. 3 C). A corresponding increase in IFN-β level was observed in NSD3-transfected cancer cells upon VSV infection (Fig. S3 G). NSD3-deficient PMs also produced lower levels of IL-6 and TNF as well as IL-8 and COX-2 upon viral infection (Fig. S4, A–C), which could be attributed to the impaired activation of p65 but not MAPK pathway by NSD3 (Fig. S4 D). Importantly, NSD3-deficient mice were more susceptible to VSV infection, as demonstrated by a lower level of IFN-β in serum and organs (Fig. 3, D and E), the increased VSV replication and titers in organs (Fig. 3, F and G), more obvious infiltration of inflammatory cells and more severe tissue damage in lung (Fig. 3 H), as well as shorter survival and higher mortality (Fig. 3 I), as compared with littermate control mice. Therefore, NSD3 was critical for the induction of type I IFNs and antiviral innate response.

## NSD3 enhances transcription activity of IRF3 dependent on K366 monomethylation

We wondered what the effect was of NSD3-mediated IRF3 methylation on the transcriptional activity of IRF3. As shown in Fig. 4 A, IRF3-driven *Ifnb* activation was obviously enhanced by NSD3 upon viral infection. Of all the NSD3 truncations, transfection of the SET domain–deficient mutants that lack methyltransferase activity, including ΔPWWP2+SET+PHD4 and ΔSET+PHD4, and the PWWP1 domain–deficient mutants that lack IRF3-interacting ability, including ΔPWWP1 and ΔPWWP1+PHD1–3, abolished NSD3-mediated IRF3 activation, whereas the deletion of PHD4 domain (loss of the ability for histone recognition; He et al., 2013) hardly affected the NSD3-mediated IRF3 activation (Fig. 4 B). So, NSD3-promoted IRF3 activation was dependent on both the IRF3-binding ability of PWWP1 domain and the methyltransferase activity of the SET domain.

As NSD3 regulates gene transcription mostly through methylation of H3K36, we then investigated whether NSD3 regulates *Ifnb* activation by targeting H3K36 in viral infec-

**3600**

NSD3 methylates IRF3 to promote innate immunity | Wang et al.
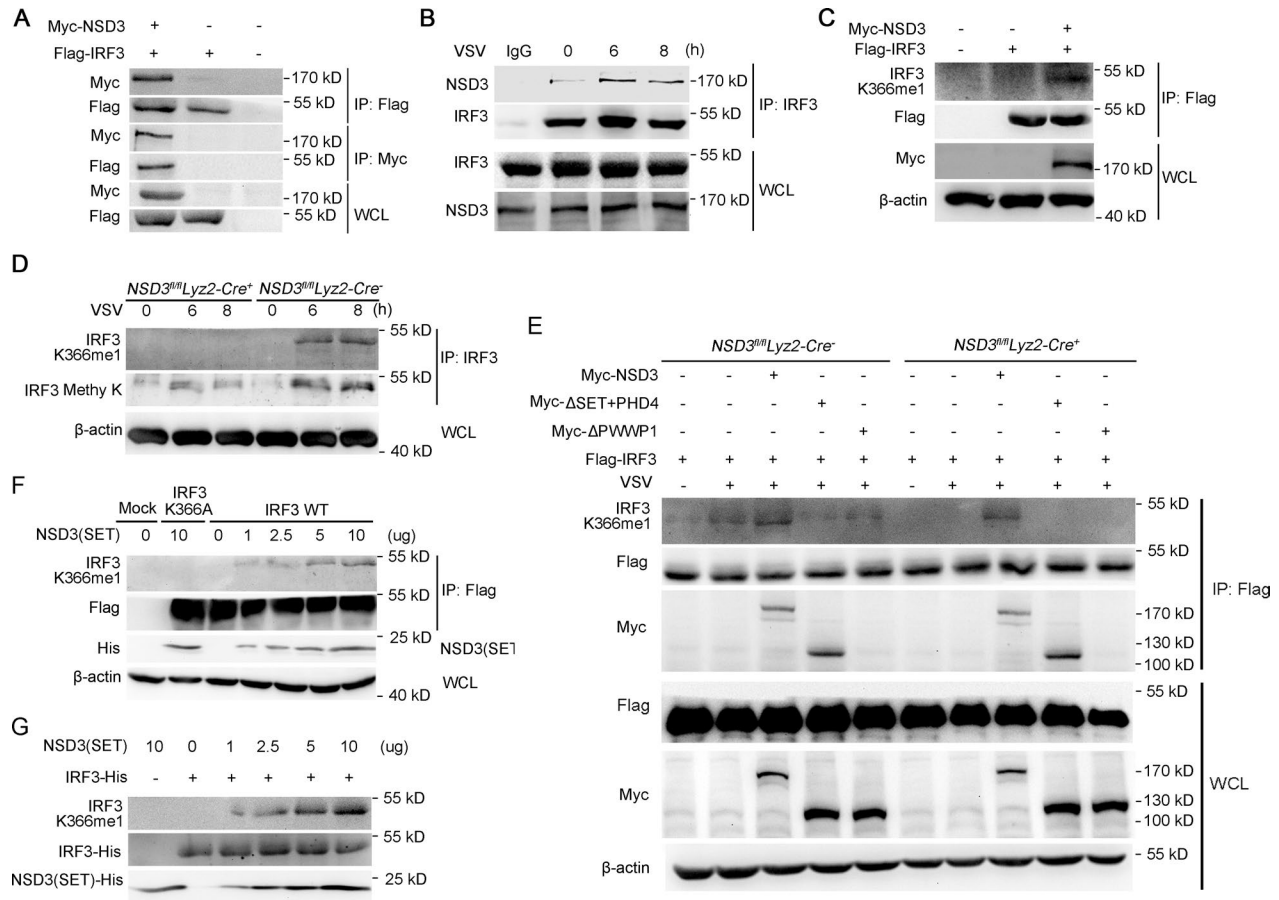
Figure 2. **NSD3 directly binds to IRF3 and methylates K366 of IRF3.** (A) HEK293T cells were cotransfected with Myc-NSD3– and FLAG-IRF3–expressing plasmids and were infected 24 h later with VSV (1 MOI) for 8 h. Cell lysates were subjected to IP with anti-Myc or anti-FLAG and then immunoblotted with the indicated antibodies. (B) Mouse PMs were infected with VSV (1 MOI) for the indicated times. Cell lysates were subjected to IP with anti-IRF3 antibody and then immunoblotted with the indicated antibodies. (C) HEK293T cells were cotransfected with FLAG-IRF3 and/or Myc-NSD3 expression vectors and infected 24 h later with VSV (1 MOI) for 8 h. K366 methylation was immunoprecipitated using anti-FLAG antibody and then detected by immunoblot analysis. (D) PMs derived from $NSD3^{fl/fl}lyz2$-$cre^+$ or $NSD3^{fl/fl}lyz2$-$cre^-$ mice were infected by VSV (1 MOI), and K366 methylation was immunoprecipitated using anti-IRF3 antibody and then detected by immunoblot analysis. (E) MEF cells from $NSD3^{fl/fl}lyz2$-$cre^+$ or $NSD3^{fl/fl}lyz2$-$cre^-$ mice were transfected with WT NSD3 or NSD3 mutants by FuGENE HD transfection reagent for 24 h and then infected with VSV (1 MOI) for 8 h and subjected to IP and immunoblot analysis for K366 methylation. (F) Immunoprecipitated IRF3 from HEK293T cells overexpressing FLAG-IRF3 was used as substrate and subjected to in vivo methylation kinase assay using purified NSD3(SET) protein. Immunoblot assay was performed with the indicated antibodies. (G) Purified His-tagged IRF3 protein was used as substrate in the in vitro kinase assay as in F. Immunoblots are representative of three independent experiments. WCL, whole cell lysate.

tion. As shown in Fig. 4 C, the abundance of H3K36me3 but not H3K36me1 and H3K36me2 to *Ifnb* gene promoter was detected in virus–infected macrophages; however, NSD3 had hardly any effect on the H3K36me3 levels of *Ifnb* gene promoter, suggesting that NSD3–mediated promotion of IFN-β production was independent of H3K36 methylation.

We further investigated the crucial role of IRF3 K366 methylation in NSD3–mediated IFN-β production. As shown in Fig. 4 D, NSD3–mediated promotion of IRF3–driven *Ifnb* activation was significantly reduced in the presence of K366A–mutated IRF3. Besides, the IFN-β production was less in IRF3–deficient MEF cells transfected with NSD3 and IRF3(K366A) than in those with NSD3 and WT IRF3; however, transfection with the K366 methylation mimic

IRF3(K366F) alone had the same effect on NSD3–mediated IFN-β production as that with NSD3 and WT IRF3 (Fig. 4 E), which further confirms that NSD3–mediated IRF3 K366 methylation is responsible for promotion of IFN-β production.

Collectively, these data show that NSD3 enhances IRF3 activation by its methyltransferase activity targeting on K366 residue of IRF3.

## NSD3 maintains IRF3 phosphorylation by preventing protein phosphatase PP1cc–mediated IRF3 dephosphorylation

How does NSD3–mediated methylation of IRF3 regulate IRF3 transcriptional activity? IRF3 has been shown to be regulated by distinct PTMs such as phosphorylation, ubiquitination (Deribe et al., 2010; Liu et al., 2016), and, as shown in
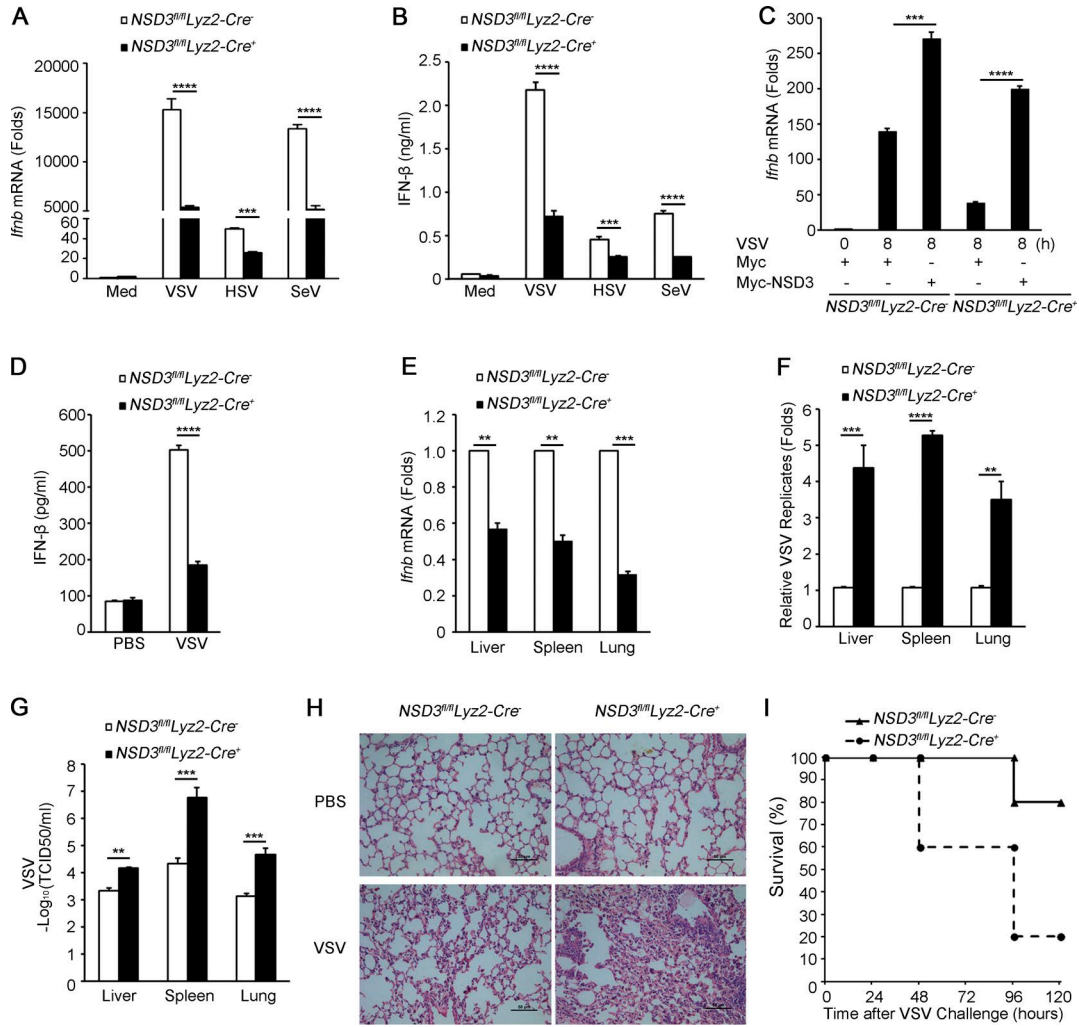
Figure 3. **Deficiency of NSD3 impairs antiviral innate immune response in vivo.** (A and B) *Ifnb* mRNA expression (A) and IFN-β production in supernatants (B) of *NSD3^fl/fl^lyz2-cre^+^* or *NSD3^fl/fl^lyz2-cre^−^* mouse–derived PMs infected with VSV (1 MOI), HSV (10 MOI), or Sendai virus (SeV; MOI = 1) for 12 h were assayed by Q-PCR and ELISA. (C) PMs derived from *NSD3^fl/fl^lyz2-cre^+^* or *NSD3^fl/fl^lyz2-cre^−^* mice were electronically transfected with NSD3 plasmid and infected 24 h later with VSV (1 MOI) for 8 h. *Ifnb* mRNA expression was determined by Q-PCR analysis. (D–G) *NSD3^fl/fl^lyz2-cre^+^* or *NSD3^fl/fl^lyz2-cre^−^* mice were challenged by intraperitoneal injection of VSV (5 × 10⁷ PFU/g; *n* = 5 per group). 18 h later, IFN-β in sera was detected by ELISA (D). IFN-β mRNA (E) and VSV replication (F) and titers (G) were assessed by Q-PCR. (H) Lung sections were subjected to pathological analysis by hematoxylin and eosin staining. Bars, 50 µm. Images are representative of two independent experiments. (I) Survival of mice (*n* = 6 per genotype) were monitored for the indicated periods (Wilcoxon test). (A–G) Data are mean ± SEM and representative of three independent experiments (unpaired, two-tailed Student's *t* test). **, P < 0.01; ***, P < 0.001; ****, P < 0.0001. Med, control medium.

this study, lysine methylation. Lysine methylation was shown to modulate phosphorylation in regulating activity of signaling molecules such as AKT (Yoshioka et al., 2016). However, the interplay between methylation and phosphorylation in the control of innate TFs and antiviral immunity remains elusive. We thus examined the effect of NSD3 on the phosphorylation of IRF3. VSV-triggered IRF3 phosphorylation at Ser388 was decreased in NSD3-deficent PMs as compared with WT PMs (Fig. 5 A). However, NSD3 deficiency did not affect VSV-triggered homodimerization (Fig. 5 B) or nuclear translocation of IRF3 (Fig. 5 C).

Noticeably, NSD3 deficiency–mediated decrease of IRF3 phosphorylation was localized only in the nucleus (Fig. 5 D). Interestingly, the interaction of NSD3 and K366-methylated IRF3 was detected only in the nuclear compartment (Fig. 5 E), indicating that NSD3 mediated IRF3 methylation in the nucleus. Usually, phosphorylated IRF3 translocates to the nucleus, where IRF3 exerts its transcriptional activation, and then IRF3 would be dephosphorylated to maintain the balance of its transcriptional activity. Thus, the role of NSD3–mediated IRF3 K366 methylation in IRF3 phosphorylation was investigated. We
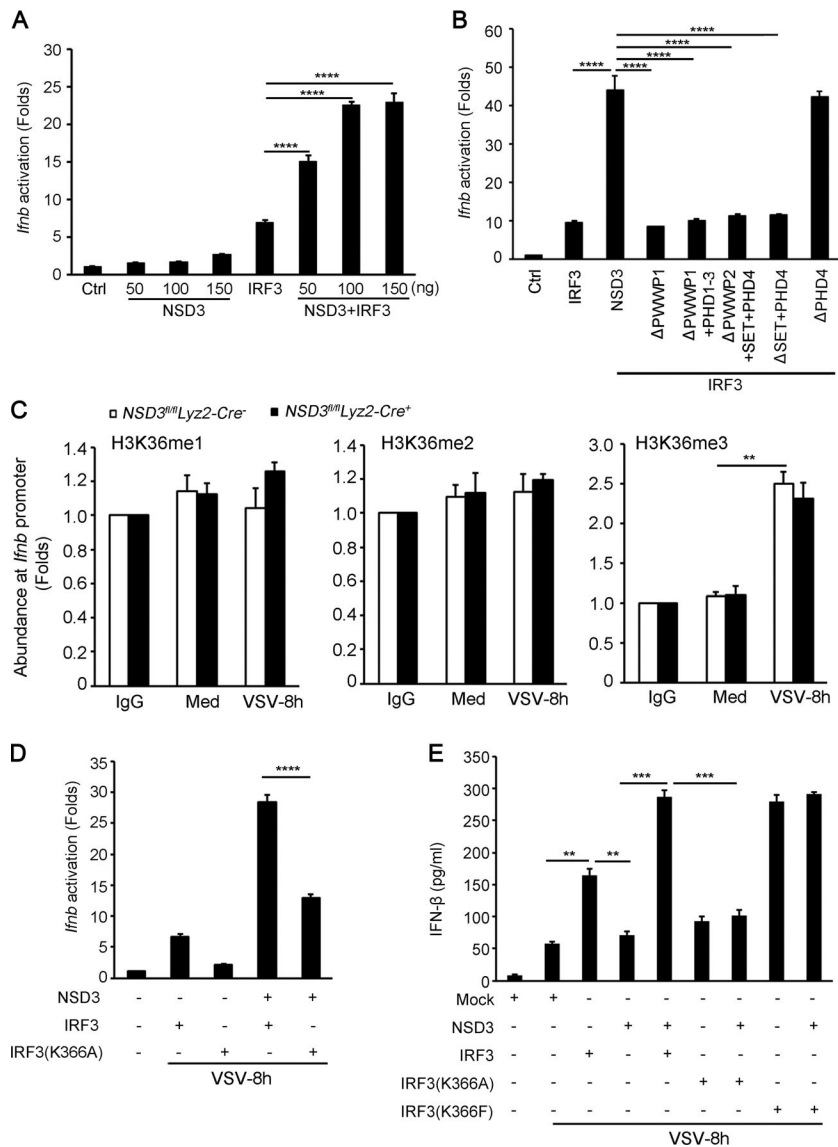
Figure 4. **NSD3 enhances IRF3 transcriptional activity.** (A and B) Luciferase activity assay in lysates of VSV-infected HEK293T cells cotransfected with different doses of NSD3-expressing plasmids with or without IRF3 plasmid (A) and transfected with NSD3 or its transcant mutants together with IRF3 (B) with *Ifnb* Luc reporter plasmid, and pTK-Renilla-luciferase. (C) ChIP analysis of H3K36 methylation (including H3K36me1, H3K36me2, and H3K36me3) to the *Ifnb* promoter in VSV-infected PMs derived from *NSD3^{fl/fl}lyz2-cre^+* or *NSD3^{fl/fl}lyz2-cre^−* mice. Med, control medium. (D) HEK293T cells transfected with NSD3 or its transcant mutants together with IRF3 or IRF3 mutants, Ifnb Luc reporter plasmid, and pTK-Renilla-luciferase. 24 h later, the cells were infected with VSV (1 MOI) for 8 h, and *Ifnb* luciferase activity in the cell lysates was analyzed. (E) IFN-β production in MEF cells derived from IRF3-deficient mice transfected with NSD3 and IRF3 or IRF3(K366A) or IRF3(K366F) was detected by ELISA. Mock, NSDE empty control vector. Data are mean ± SEM and representative of three independent experiments (A and B, one-way ANOVA, $n$ = 4–6 per group; C–E, unpaired, two-tailed Student's $t$ test). **, P < 0.01; ***, P < 0.001; ****, P < 0.0001.

found IRF3 phosphorylation was reduced in HEK293T cells cotransfected with NSD3 and K366A mutant as compared with NSD3 and IRF3 (Fig. 5 F). The similar result was also observed in IRF3-deficient MEF cells cotransfected with NSD3 and IRF3 or IRF3(K366A) (Fig. 5 G). The purified NSD3(SET) protein also could methylate the immunoprecipitated IRF3(S388A), a mutant of Ser388 phosphorylation of IRF3 (Fig. 5 H), indicating that IRF3 phosphorylation has no effect on NSD3-mediated IRF3 K366 methylation. These results suggest that the NSD3-mediated increase of IRF3 phosphorylation was dependent on NSD3-mediated methylation of K366.

Protein phosphatases such as SHP1, SHP2, and PP1, etc., are involved in the regulation of IRF3 activity via dephosphorylation (An et al., 2006, 2008; Gu et al., 2014). Among them, SHP1 and SHP2 were localized in cytoplasm but not the nucleus in macrophages with or without viral stimulation;

however, PP1 was localized both in the cytoplasm and nucleus (Fig. 6 A). Thus, PP1, which was reported as a phosphatase binding to and regulating IRF3 in the VSV-triggered innate response (Gu et al., 2014), was more likely to be involved in the NSD3-mediated regulation of IRF3 phosphorylation. Interestingly, the binding of IRF3 to PP1cc, an isoform of the PP1-gamma catalytic subunit, was reduced, whereas the phosphorylation of IRF3 was increased in HEK293T cells overexpressing NSD3 (Fig. 6, B and C). Accordingly, IRF3 phosphorylation was reduced, whereas the association of IRF3 with PP1cc was increased in NSD3-deficient PMs infected with VSV (Fig. 6 D). Moreover, the impaired phosphorylation of IRF3 and decreased production of IFN-β in NSD3-deficient PMs induced by VSV infection were almost reversed by PP1cc silencing (Fig. 6, E and F). These results suggest that NSD3 decreases the binding of IRF3 and PP1cc, preventing dephosphorylation of IRF3 by PP1cc and con-
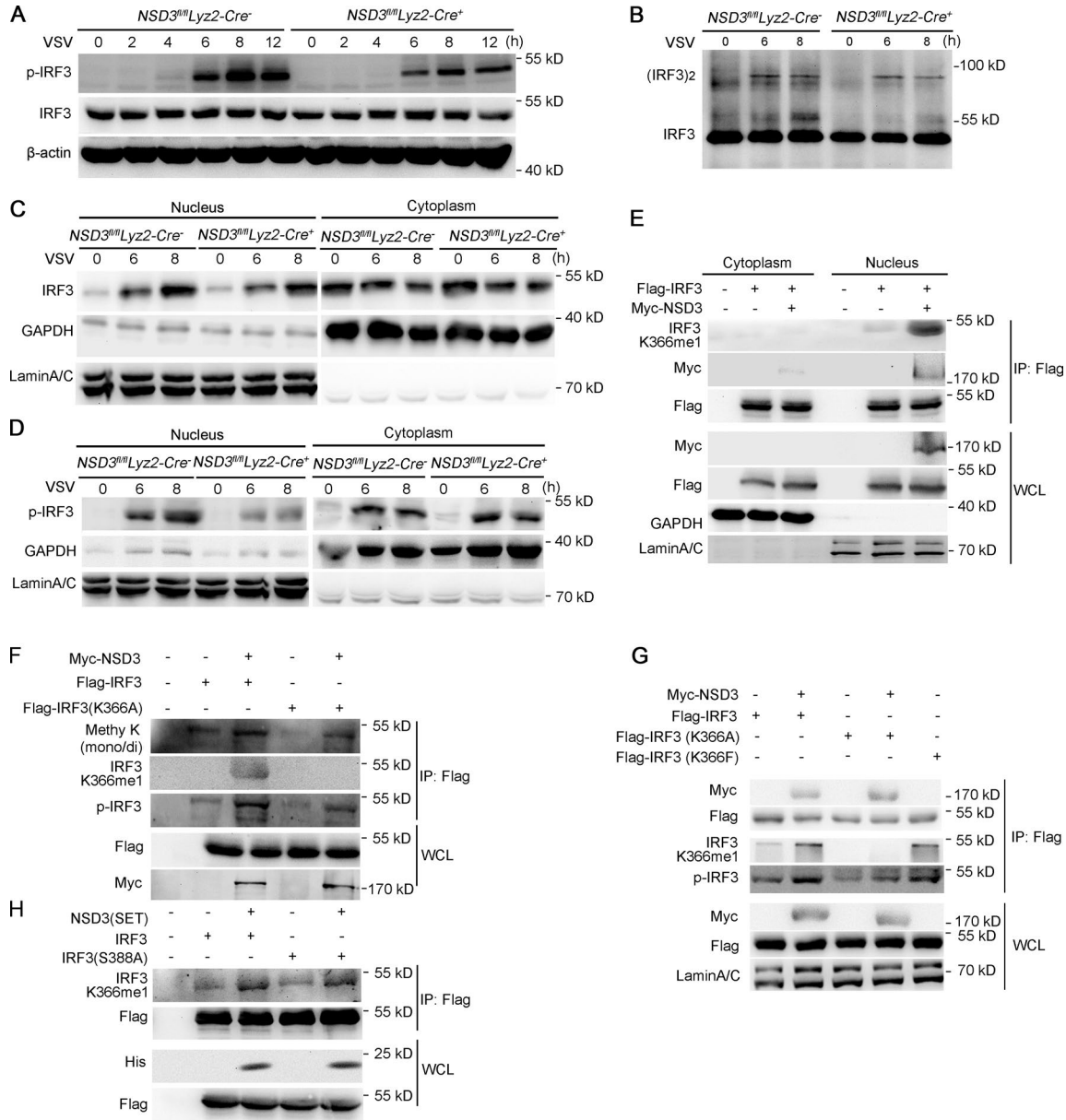
Figure 5. **NSD3 increases viral infection–triggered IRF3 phosphorylation in nucleus dependent on K366 methylation.** (A–D) PMs from *NSD3^{fl/fl}lyz2-cre^+* or *NSD3^{fl/fl}lyz2-cre^−* mice were infected with VSV (1 MOI) for the indicated times. IRF3 phosphorylation in total cell lysates (A), IRF3 dimerization (B), nuclear translocation (C), and IRF3 phosphorylation (D) in nucleus or cytoplasm fractions were detected by immunoblot analysis. (E) HEK293T cells were cotransfected with NSD3 together with WT IRF3. 24 h later, cells were infected with VSV (1 MOI) for 8 h. The cellular extracts were divided into nuclear and cytosolic fractions and subjected to IP and immunoblot analysis for K366 methylation. (F and G) HEK293T cells (F) and MEF cells from IRF3-deficient mice (G) were cotransfected with NSD3 together with WT IRF3 or mutants. 24 h later, the cells were infected with VSV (1 MOI) for 8 h and subjected to IP and immunoblot analysis for K366 methylation and IRF3 phosphorylation. (H) Immunoprecipitated IRF3 from HEK293T cells overexpressing IRF3 or IRF3 mutants (IRF3 K388A) was used as substrate and subjected to in vitro methylation kinase assay using purified NSD3(SET) protein. Immunoblot analysis was performed for K366 methylation. Immunoblots are representative of three independent experiments. WCL, whole cell lysate.

sequently resulting in maintenance of IRF3 phosphorylation and IFN-β production.

We then investigated how NSD3-mediated IRF3 K366 methylation prevents the association of IRF3 and PP1cc. As shown in Fig. 6 G, the binding of IRF3 to PP1cc was sig-

nificantly increased in HEK293T cells overexpressing NSD3 and IRF3(K366A) compared with those overexpressing NSD3 and IRF3. Of note, minor interaction was observed in HEK293T cells overexpressing K366–methylated mimic, IRF3(K366F). In vitro, NSD3(SET)–mediated methylation of

3604

NSD3 methylates IRF3 to promote innate immunity | Wang et al.
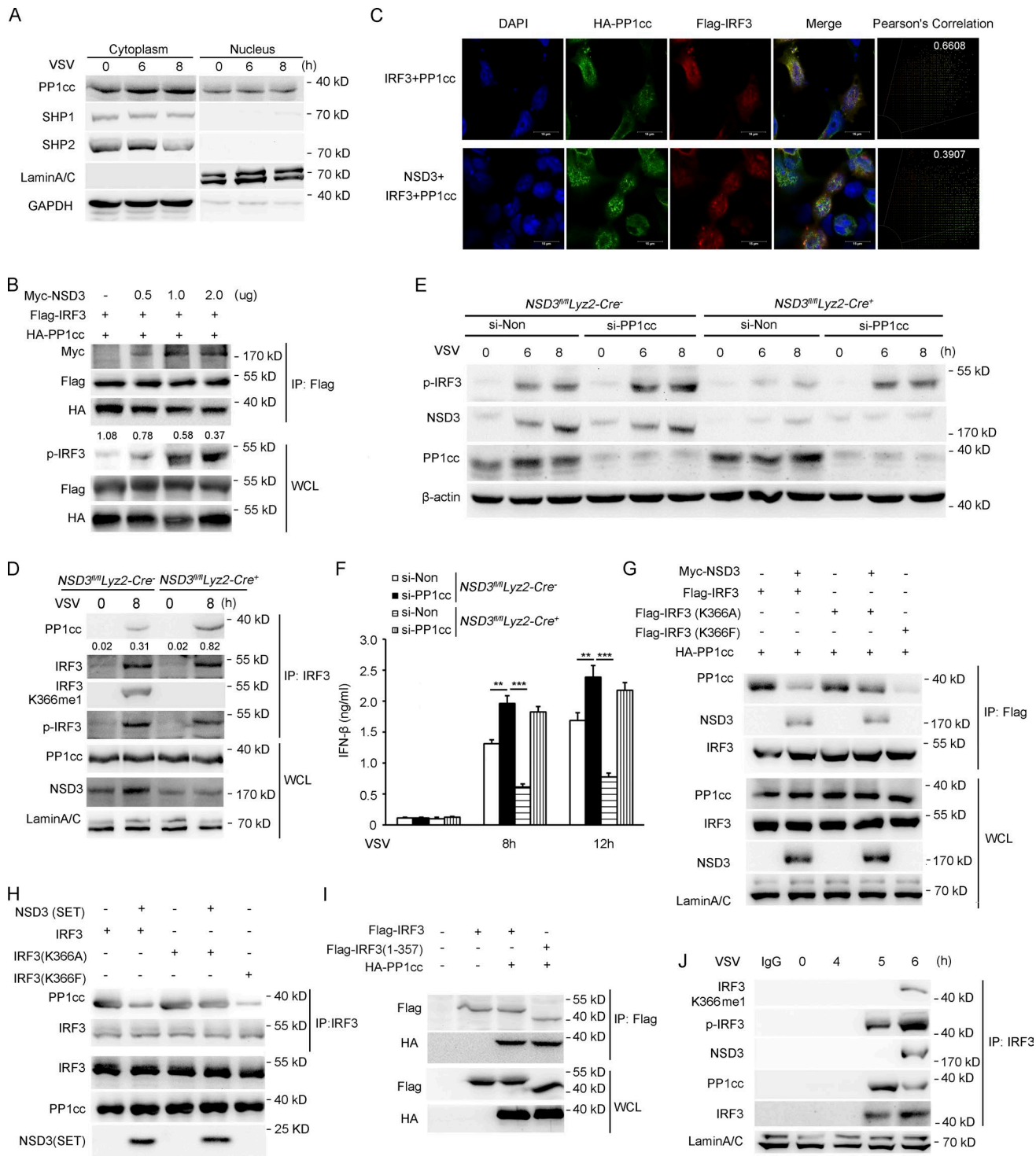
Figure 6. **NSD3–mediated IRF3 K366 methylation disrupts the association between IRF3 and PP1cc.** (A) PMs were infected with VSV (1 MOI) for the indicated times and subjected to immunoblot analysis by the indicated antibodies. (B and C) HEK293T cells were transiently transfected with FLAG-IRF3 together with Myc-NSD3 or HA-PP1cc. 24 h later, the cells were infected with VSV (1 MOI) for the indicated times and subjected to IP and immunoblot analysis (B) and confocal microscopy (C) for the interaction of IRF3 and PP1cc and IRF3 phosphorylation in nucleus; numbers below lanes indicate densitometry of interacted PP1cc relative to that of total HA-PP1cc. Bars, 15 μm. (D) PMs from *NSD3$^{fl/fl}$lyz2-cre$^+$* or *NSD3$^{fl/fl}$lyz2-cre$^-$* mice were infected with VSV (1 MOI) for 8 h and then subjected to IP and immunoblot analysis for the interaction of IRF3 and PP1cc and IRF3 phosphorylation in nucleus; numbers below lanes indicate densitometry of interacted PP1cc and total NSD3 relative to that of LaminA/C. (E and F) PMs from *NSD3$^{fl/fl}$lyz2-cre$^+$* or *NSD3$^{fl/fl}$lyz2-cre$^-$* mice were transfected with PP1cc siRNA for 48 h and infected with VSV (1 MOI) for 8 h and then subjected to immunoblot analysis (E) and ELISA analysis (F).

purified IRF3 protein, but not IRF3(K366A), dramatically decreased the PP1cc binding ability of IRF3, whereas purified IRF3(K366F) alone exhibited much less ability to bind PP1cc (Fig. 6 H). In addition, IRF3(1–357) also bound to PP1cc, suggesting that the PP1cc-binding domain of IRF3 does not overlap with K366 site (Fig. 6 I).

We further explore the spatial–temporal dynamics by which IRF3 was modified. As shown in Fig. 6 J, the interaction between IRF3 and PP1cc occurred at 5 h after VSV infection in PMs, which preceded the interaction between IRF3 and NSD3 and IRF3 methylation at 6 h, with the decrease of binding of PP1cc and IRF3. These results indicated that NSD3-mediated IRF3 methylation promoted the disassociation of IRF3 and PP1cc.

Therefore, we propose a working model of NSD3 in promoting antiviral innate response that NSD3-mediated IRF3 K366 methylation maintains phosphorylation of IRF3 by preventing IRF3 dephosphorylation via disrupting the association of IRF3 and PP1cc (as illustrated in Fig. S5).

## DISCUSSION

IRF3 is a key TF, activating the expression of type I IFNs upon viral infection, which modulates various aspects of biological and immunological pathways. We found that lysine methyltransferase NSD3 interacts with and directly monomethylates IRF3 in the nucleus, leading to the enhanced IRF3 transcriptional activity and antiviral immune responses. Thus, we describe a new IRF3 regulatory pathway through lysine methylation upon virus infection, revealing a previously unknown mechanism for immune regulation that involves NSD3-mediated methylation, as well as cross talk between methylation and phosphorylation of IRF3.

Despite considerable evidence that phosphorylation and dephosphorylation are linked to the function and stability of IRF3 (Li et al., 2016a), relatively little is known about how other PTMs (such as methylation) regulate its function. The results presented in our study have demonstrated that IRF3 was subjected to an additional PTM, methylation, through its interaction with NSD3. In particular, viral infection induces methylation of IRF3 at K366, and such modification is essential for the virus-triggered induction of type I IFNs. To the best of our knowledge, NSD3 is the first methyltransferase identified so far that directly catalyzes methylation of IRF3. We show that K366 is a crucial residue of IRF3,

which is targeted by NSD3 for IRF3-mediated production of IFN-β. IRF3 K366 is conserved among several species, including mouse, rat, and pig, but not in human (a corresponding residue is arginine). Whether the arginine residue in human IRF3 could be methylated by certain arginine methyltransferases or whether there exist other lysine sites to be methylated by NSD3 needs further investigation. In addition, methylation-defective K381A mutation is also capable of abolishing IRF3-driven *Ifnb* activation. Thus, we can't rule out the possibility that NSD3 could also methylate other sites of IRF3 (e.g., K381). Further investigations may be required to systematically investigate the methylation of IRF3 by NSD3 and to unveil the physiological importance of NSD3 methylation in more detail.

An important issue for the current research on antiviral immunity is the spatiotemporal dynamics by which IRF3 is modified. Our results here have established that NSD3 deficiency hardly has any effect on VSV-triggered homodimerization or the nuclear translocation of IRF3 and that NSD3 binds to IRF3 and disrupts the interaction of IRF3 with PP1cc in nucleus. This is consistent with previous reports that the NF-κB p65 is significantly associated with histone-modifying enzymes F-box and leucine-rich repeat protein 11 (FBXL11) or NSD1 only after it's released from IκB and translocates into the nucleus (Lu et al., 2010). In addition, EZH2 may bind preferentially to promoter-bound STAT3 phosphorylated homodimers rather than to STAT3 homodimers that are not associated with promoters (Dasgupta et al., 2015). These data may support the possibility that only when inducible TFs translocate into the nucleus and gain access to specific promoters, where the local chromatin remodeling machinery is active, may their methylation occur. However, we have shown that NSD3-mediated promotion of IFN-β production is independent of NSD3-mediated H3K36 methylation. Therefore, it will be intriguing to decipher the mechanisms underlying the selectivity and cross talk of histone and nonhistone methylation of NSD3.

The interplay and cross talk between phosphorylation and methylation events have become a recurrent theme in the PTM control of cellular signaling. TFs, which are often modified by multiple types of PTMs, provide a salient case of PTM cross talk. In most of the TFs such as forkhead box protein O1 (FOXO1; Yamagata et al., 2008), NF-κB (Chang et al., 2011; Levy et al., 2011), and retinoblastoma protein (RB; Carr et al.,

2011), direct interactions between neighboring phosphorylation and methylation sites provide a mutually exclusive methylation–phosphorylation switch (Sabbattini et al., 2014), resulting in interconversion between different activation forms of the TF. Interestingly, our findings here reveal that IRF3 methylation by NSD3 at K366 maintains IRF3 phosphorylation and enhances its transcriptional activity. Similarly, Tyr (Y705) phosphorylation and activation of STAT3 in glioblastoma stem cell–like cells are positively regulated by STAT3 methylation on K180, performed by EZH2 (Kim et al., 2013). In addition, we found that the NF-κB subunit p65 might be another methylation substrate of NSD3 because NSD3 deficiency decreased the phosphorylation of p65 and the expression of its targets (e.g., TNFα, IL-6, COX-2, and IL-8). Although these might be derived from distinct mechanisms, our study raises several noteworthy issues, e.g., what is the molecular basis of the cross-regulation of IRF3 by NSD3-mediated K366 methylation and PP1cc-mediated dephosphorylation? Lysine residues of protein are often exposed on the peptide surface, determining the protein–protein interactions and protein PTMs (Polevoda and Sherman, 2007). We speculated that NSD3-mediated K366 monomethylation may alternate the conformation of IRF3, resulting in disassociation of IRF3 and PP1cc, thus maintaining IRF3 phosphorylation. Of note, our results from MS and luciferase reporter assay also reveal another methylation site (K381) that positively regulates IRF3-mediated *Ifnb* transcriptional activation, suggesting the activity of IRF3 may be regulated by multiple and interacting modifications.

The IRF3 activation is a pivotal effector event leading to diverse regulatory effects in a context-specific manner. Based on our findings, we suggest the following model for NSD3-promoted activation of IRF3 in the antiviral innate immune response: upon virus infection, phosphorylated IRF3 translocates into the nucleus, where the inducible expressed NSD3 interacts with and monomethylates IRF3 at K366 site, disrupts the association of PP1cc and IRF3, and subsequently maintains IRF3 phosphorylation in the nucleus and thus promotes type I IFN production in the antiviral innate responses. In conclusion, our study provides a new PTM layer of IRF3 that can enhance antiviral innate immunity and may provide a therapeutic strategy to control viral infectious diseases.

## MATERIALS AND METHODS
### Animal experiments
The generation of *NSD3*^{fl/fl} mice was as follows: BAC recombineering was used to generate loxp-flanked *NSD3* mice (*NSD3*^{fl/fl}), and two floxps were located at the upstream intron of the 16th exon and the downstream intron of the 17th exon, respectively, and Neo gene flanked with Frt was used to screen out the recombined embryonic stem cell clones. Targeted embryonic stem cells were identified by Southern blot and were injected into C57BL/6 blastocysts to generate high–percentage chimeras. *NSD3* floxed allele was obtained after deletion of the *Neo* gene by cross-ing between *NSD3* chimeras with B6; SJL-Tg (ACTFLPe) 9205Dym/J mice (003800; Jackson Laboratory). To specifically delete *NSD3* in macrophages, *NSD3*-floxed alleles were crossed with SJL-Tg (ACTFLPe) and B6.129P2-*Lyz*[tm1(cre)Ifo]/J mice (004781; Jackson Laboratory). The genotyping primers were TgLacZ-F, 5′-CAAACTGGCAGA TGCACGGTTAC-3′; TgLacZ-R, 5′-CAGTACAGCGCG GCTGAAATC-3′; NSD3-F, 5′-GCGTGAAAGCAAGGA GGC-3′; and NSD3-R 5′-GGGTGACCATCGGAGCAT-3′. IRF3-deficient mice were provided by T. Taniguchi from the University of Tokyo, Tokyo, Japan. Male C57BL/6J mice (6–8 wk) were from Joint Ventures Sipper BK Experimental Animal Company. Mice were bred in pathogen–free conditions. All animal experiments were undertaken in accordance with the National Institutes of Health Guide for the Care and Use of Laboratory Animals with approval of the Scientific Investigation Board of Second Military Medical University, Shanghai, China.

### Antibodies and reagents
Antibodies against phosphorylated IRF3 (Ser396) (4947), IRF3 (4302), LaminA/C (4777S), GAPDH (3683S), HA tag (3724), Myc tag (2272), FLAG tag (2368), SHP1 (3759), SHP2 (3397), His tag (12698), and horseradish peroxidase–coupled secondary antibodies (14031) were from Cell Signaling Technology. Antibodies against β-actin (sc-130656) and GST antibody (sc-138) were from Santa Cruz. Anti–calmodulin-binding protein epitope tag antibody (07–482) was from Millipore; Dynabead MyOne Streptavidin C1 (65002) was from Invitrogen; anti–NSD3 (ab137430), histone H3 (monomethyl K36) (anti–H3K36me1) antibody (ab9048), histone H2 (dimethyl K36) (anti–H3K36me2) antibody (ab9049), and histone H3 (trimethyl K36) (H3K36me3) antibody (ab9050) were from Abcam. Antimono-/dimethylated lysine (PTM-602) was from PTM Biolab; anti–mouse F4/80 PE (12-4801) and anti–mouse CD11b APC (17-0112) used for FACS were from BD; anti–Myc-agarose (A7470) and anti–FLAG-agarose (M8823) used for IP were from Sigma-Aldrich. The polyclonal antibody against IRF3 K366 monomethylation (IRF3 K366me1) was custom produced by Abmart. IRF3-his and NSD3(SET)-his fusion proteins were custom produced by Detai Biologics. S-(5′-Adenosyl)-ʟ-methionine chloride dihydrochloride (1A7707) was from Sigma-Aldrich. Protein G agarose (20397) used for IP was from Pierce; chromatin IP (ChIP)–grade protein G magnetic beads (9006) and cell lysis buffer (9803) were from Cell Signaling Technology. LPS (0111:B4), CpG, and PolyI:C have been described previously (Wang et al., 2013). Ammonium pyrrolidinedithiocarbamate was from Sigma-Aldrich (5108-96-3). HSV was a gift from Q. Li (Chinese Academy of Sciences, Beijing, China), VSV was a gift from W. Pan (Second Military Medical University, Shanghai, China), and Sendai virus was a gift from B. Sun (Chinese Academy of Sciences, Shanghai, China). Influenza A virus (H1N1) was from ATCC (VR-95).

## Cell culture and transfection

HEK293T and RAW264.7 cell lines were from ATCC. Thio-glycolate-elicited mouse PMs were isolated and cultured as described previously (Zhang et al., 2015). Primary MEF cells were isolated form IRF3-deficient embryos. Stable overexpression of TAP-tagged IRF3 cells (TAP-RAW264.7 cells) were established by using interplay TAP-expressing system (Merck) containing a calmodulin-binding protein, and strepta-vidin–binding protein epitopes in TAP tag were established by our laboratory. All cells were cultured in endotoxin-free DMEM (Gibco), supplemented with 10% FCS (Invitrogen), 5 mg/ml penicillin (Gibco), and 10 mg/ml streptomycin (Gibco).

For transient transfection of plasmids in HEK293T cells and MEF cells, jetPEI reagent (PolyPlus) was used according to the manufacturer's instructions. For transient transfection of plasmids in PMs, nuclear transfection was performed by using an Amaxa P3 Primary Cell 4D–Nucleofector X kit (Lonza) according to the manufacturer's instructions.

## Real–time quantitative PCR (Q–PCR)

Total RNA was extracted and subjected to Q-PCR as described previously (Li et al., 2016b). The primers used for murine *Ifnb* were 5′-CAGCTCCAAGAAAGGACGAAC-3′ (sense) and 5′-GGCAGTGTAACTCTTCTGCAT-3′ (antisense). Primers used for murine TNF were 5′-GACGTG GAACTGGCAGAAGAG-3′ (sense) and 5′-TTGGTGGTT TGTGAGTGTGAG-3′ (antisense). Primers used for murine IL-6 were 5′-TAGTCCTTCCTACCCCAATTTCC-3′ (sense) and 5′-TTGGTCCTTAGCCACTCCTTC-3′ (antisense). Primers used for β-actin were 5′-AGTGTGACG TTGACATCCGT-3′ (sense) and 5′-GCAGCTCAGTAA CAGTCCGC-3′ (antisense). Data were normalized by the level of β-actin expression in each sample.

## ELISA

IFN-β, TNF, and IL-6 levels in the supernatants or sera were measured by mouse IFN-β ELISA kit (PBL Biomedical Laboratories), TNF, or IL-6 ELISA kit (R&D).

## Plasmid constructs and transfection

Expression vectors encoding Myc-tagged NSD3 and Myc-tagged IRF3 were constructed by PCR cloning into pcD-NA3.1-Myc eukaryotic expression vector and FLAG-tagged IRF3 into pcDNA3.1-FLAG vector, respectively. Mutants and truncations of IRF3 and NSD3 were generated by PCR-based amplification. The primers are shown in Table S2. Each recombinant expression vector was transiently transfected into HEK293T cells with jetPEI reagents according to the manufacturer's instructions and was transiently transfected into PMs by Nucleofector kit.

## Co–IP and immunoblot analysis

The cellular extraction was measured by BCA assay (Pierce). IP and immunoblot analysis were performed as described previously (Li et al., 2016b).

## Apoptosis analysis

The cellular apoptosis was performed as described by Hou et al. (2014).

## MS analysis of lysine methylation

MS analysis was performed as described by Chen et al. (2017). TAP-IRF3 RAW264.7 cells were infected with VSV for 8 h and then lysed. 1 mg total protein was immunoprecipitated with TAP antibody–conjugated magnetic beads. TAP-overexpressing cells were used as control. After Coomassie blue staining, the IRF3-specific band with intensive signal compared with TAP control was cut and followed with reverse-phase nanospray liquid chromatography–tandem MS analysis. The spectra from tandem MS were automatically used for searching against the nonredundant International Protein Index mouse protein database (version 3.72) with the BioWorks browser (rev.3.1; Thermo Fisher).

## Luciferase reporter gene assay

The transcriptional activity of IRF3 was examined by measuring Ifnb transcription using luciferase reporter gene assay as described previously (Wang et al., 2013).

## ChIP assay

ChIP assays were conducted with a ChIP assay kit (Millipore) according to the manufactures' protocol (Wang et al., 2013).

## In vitro assay for methylated kinase

In vitro analysis of methylation of IRF3 by NSD3 was performed as described previously (Levy et al., 2011). HEK293T cells were transfected with FLAG-IRF3 vector, and cellular lysates (300 μg) were subjected to IP with anti-Flag antibody. The anti-FLAG immunoprecipitant or recombinant IRF3-his protein (1 μg) was incubated with recombinant NSD3(SET)-his protein and 0.1 mM S-adenosyl-methionine in the kinase buffer containing 50 mM Tris-HCl, pH 8.0, 10% glycerol, 20 mM KCl, 5 mM $MgCl_2$, and 1 mM PMSF at 30°C overnight.

## Statistical analysis

Statistical significance between two groups was determined by unpaired two-tailed Student's *t* test or one-way ANOVA. Differences were considered to be significant when $P < 0.05$. *, $P < 0.05$; **, $P < 0.01$; ***, $P < 0.001$; ****, $P < 0.0001$. For mouse survival study, Kaplan-Meier survival curves were generated and analyzed for statistical significance with Prism 5.0 (GraphPad).

## Online supplemental material

Fig. S1 shows K366 methylation of IRF3 in cancer cells. Fig. S2 shows that NSD3 binds to IRF3 via its PWWP1 domain. Fig. S3 shows virus-induced NSD3 expression in macrophages. Fig. S4 shows that deficiency of NSD3 impairs virus infection–triggered inflammatory cytokine production and p65 activation in macrophages. Fig. S5 shows a working model

of NSD3-promoted activation of IRF3 in the antiviral innate immune response. Table S1 shows MS analysis of lysine-methylated residues of mouse IRF3 in VSV-infected IRF3-over-expressing cells. Table S2 shows PCR primers for expressing vectors of mutants and truncations of IRF3 and NSD3.

## REFERENCES

An, H., W. Zhao, J. Hou, Y. Zhang, Y. Xie, Y. Zheng, H. Xu, C. Qian, J. Zhou, Y. Yu, et al. 2006. SHP-2 phosphatase negatively regulates the TRIF adaptor protein-dependent type I interferon and proinflammatory cytokine production. *Immunity.* 25:919–928. https://doi.org/10.1016/j.immuni.2006.10.014

An, H., J. Hou, J. Zhou, W. Zhao, H. Xu, Y. Zheng, Y. Yu, S. Liu, and X. Cao. 2008. Phosphatase SHP-1 promotes TLR- and RIG-I-activated production of type I interferon by inhibiting the kinase IRAK1. *Nat. Immunol.* 9:542–550. https://doi.org/10.1038/ni.1604

Biggar, K.K., and S.S. Li. 2015. Non-histone protein methylation as a regulator of cellular signalling and function. *Nat. Rev. Mol. Cell Biol.* 16:5–17. https://doi.org/10.1038/nrm3915

Carr, S.M., S. Munro, B. Kessler, U. Oppermann, and N.B. La Thangue. 2011. Interplay between lysine methylation and Cdk phosphorylation in growth control by the retinoblastoma protein. *EMBO J.* 30:317–327. https://doi.org/10.1038/emboj.2010.311

Chang, Y., D. Levy, J.R. Horton, J. Peng, X. Zhang, O. Gozani, and X. Cheng. 2011. Structural basis of SETD6-mediated regulation of the NF-kB network via methyl-lysine signaling. *Nucleic Acids Res.* 39:6380–6389. https://doi.org/10.1093/nar/gkr256

Chen, K., J. Liu, S. Liu, M. Xia, X. Zhang, D. Han, Y. Jiang, C. Wang, and X. Cao. 2017. Methyltransferase SETD2-mediated methylation of STAT1 is critical for interferon antiviral activity. *Cell.* 170:492–506.e14. https://doi.org/10.1016/j.cell.2017.06.042

Chuikov, S., J.K. Kurash, J.R. Wilson, B. Xiao, N. Justin, G.S. Ivanov, K. McKinney, P. Tempst, C. Prives, S.J. Gamblin, et al. 2004. Regulation of p53 activity through lysine methylation. *Nature.* 432:353–360. https://doi.org/10.1038/nature03117

Dasgupta, M., J.K. Dermawan, B. Willard, and G.R. Stark. 2015. STAT3-driven transcription depends upon the dimethylation of K49 by EZH2. *Proc. Natl. Acad. Sci. USA.* 112:3985–3990. https://doi.org/10.1073/pnas.1503152112

Deribe, Y.L., T. Pawson, and I. Dikic. 2010. Post-translational modifications in signal integration. *Nat. Struct. Mol. Biol.* 17:666–672. https://doi.org/10.1038/nsmb.1842

Ea, C.K., and D. Baltimore. 2009. Regulation of NF-κB activity through lysine monomethylation of p65. *Proc. Natl. Acad. Sci. USA.* 106:18972–18977. https://doi.org/10.1073/pnas.0910439106

Ezponda, T., R. Popovic, M.Y. Shah, E. Martinez-Garcia, Y. Zheng, D.J. Min, C. Will, A. Neri, N.L. Kelleher, J. Yu, and J.D. Licht. 2013. The histone methyltransferase MMSET/WHSC1 activates TWIST1 to promote an epithelial-mesenchymal transition and invasive properties of prostate cancer. *Oncogene.* 32:2882–2890. https://doi.org/10.1038/onc.2012.297

Fitzgerald, K.A., S.M. McWhirter, K.L. Faia, D.C. Rowe, E. Latz, D.T. Golenbock, A.J. Coyle, S.M. Liao, and T. Maniatis. 2003. IKKepsilon and TBK1 are essential components of the IRF3 signaling pathway. *Nat. Immunol.* 4:491–496. https://doi.org/10.1038/ni921

Gu, M., T. Zhang, W. lin, Z. Liu, R. Lai, D. Xia, H. Huang, and X. Wang. 2014. Protein phosphatase PP1 negatively regulates the Toll-like receptor- and RIG-I-like receptor-triggered production of type I interferon by inhibiting IRF3 phosphorylation at serines 396 and 385 in macrophage. *Cell. Signal.* 26:2930–2939. https://doi.org/10.1016/j.cellsig.2014.09.007

Gunawan, M., N. Venkatesan, J.T. Loh, J.F. Wong, H. Berger, W.H. Neo, L.Y. Li, M.K. La Win, Y.H. Yau, T. Guo, et al. 2015. The methyltransferase Ezh2 controls cell adhesion and migration through direct methylation of the extranuclear regulatory protein talin. *Nat. Immunol.* 16:505–516. https://doi.org/10.1038/ni.3125

Hamamoto, R., V. Saloura, and Y. Nakamura. 2015. Critical roles of non-histone protein lysine methylation in human tumorigenesis. *Nat. Rev. Cancer.* 15:110–124. https://doi.org/10.1038/nrc3884

He, C., F. Li, J. Zhang, J. Wu, and Y. Shi. 2013. The methyltransferase NSD3 has chromatin-binding motifs, PHD5-C5HCH, that are distinct from other NSD (nuclear receptor SET domain) family members in their histone H3 recognition. *J. Biol. Chem.* 288:4692–4703. https://doi.org/10.1074/jbc.M112.426148

Hou, J., Y. Zhou, Y. Zheng, J. Fan, W. Zhou, I.O. Ng, H. Sun, L. Qin, S. Qiu, J.M. Lee, et al. 2014. Hepatic RIG-I predicts survival and interferon-α therapeutic response in hepatocellular carcinoma. *Cancer Cell.* 25:49–63. https://doi.org/10.1016/j.ccr.2013.11.011

Huang, Y.C., Z. Li, X. Hyseni, M. Schmitt, R.B. Devlin, E.D. Karoly, and J.M. Soukup. 2008. Identification of gene biomarkers for respiratory syncytial virus infection in a bronchial epithelial cell line. *Genomic Med.* 2:113–125. https://doi.org/10.1007/s11568-009-9080-y

Kang, D., H.S. Cho, G. Toyokawa, M. Kogure, Y. Yamane, Y. Iwai, S. Hayami, T. Tsunoda, H.I. Field, K. Matsuda, et al. 2013. The histone methyltransferase Wolf-Hirschhorn syndrome candidate 1-like 1 (WHSC1L1) is involved in human carcinogenesis. *Genes Chromosomes Cancer.* 52:126–139. https://doi.org/10.1002/gcc.22012

Kim, E., M. Kim, D.H. Woo, Y. Shin, J. Shin, N. Chang, Y.T. Oh, H. Kim, J. Rheey, I. Nakano, et al. 2013. Phosphorylation of EZH2 activates STAT3 signaling via STAT3 methylation and promotes tumorigenicity of glioblastoma stem-like cells. *Cancer Cell.* 23:839–852. https://doi.org/10.1016/j.ccr.2013.04.008

Levy, D., A.J. Kuo, Y. Chang, U. Schaefer, C. Kitson, P. Cheung, A. Espejo, B.M. Zee, C.L. Liu, S. Tangsombatvisit, et al. 2011. Lysine methylation of the NF-κB subunit RelA by SETD6 couples activity of the histone methyltransferase GLP at chromatin to tonic repression of NF-κB signaling. *Nat. Immunol.* 12:29–36. https://doi.org/10.1038/ni.1968

Li, S., M. Zhu, R. Pan, T. Fang, Y.Y. Cao, S. Chen, X. Zhao, C.Q. Lei, L. Guo, Y. Chen, et al. 2016a. The tumor suppressor PTEN has a critical role in antiviral innate immunity. *Nat. Immunol.* 17:241–249. https://doi.org/10.1038/ni.3311

Li, X., Q. Zhang, Y. Ding, Y. Liu, D. Zhao, K. Zhao, Q. Shen, X. Liu, X. Zhu, N. Li, et al. 2016b. Methyltransferase Dnmt3a upregulates HDAC9 to deacetylate the kinase TBK1 for activation of antiviral innate immunity. *Nat. Immunol.* 17:806–815. https://doi.org/10.1038/ni.3464

Liu, J., C. Qian, and X. Cao. 2016. Post-translational modification control of innate immunity. *Immunity.* 45:15–30. https://doi.org/10.1016/j.immuni.2016.06.020

Long, L., Y. Deng, F. Yao, D. Guan, Y. Feng, H. Jiang, X. Li, P. Hu, X. Lu, H. Wang, et al. 2014. Recruitment of phosphatase PP2A by RACK1 adaptor protein deactivates transcription factor IRF3 and limits type I interferon signaling. *Immunity.* 40:515–529. https://doi.org/10.1016/j.immuni.2014.01.015

Lu, T., M.W. Jackson, B. Wang, M. Yang, M.R. Chance, M. Miyagi, A.V. Gudkov, and G.R. Stark. 2010. Regulation of NF-κB by NSD1/FBXL11-dependent reversible lysine methylation of p65. *Proc. Natl. Acad. Sci. USA.* 107:46–51. https://doi.org/10.1073/pnas.0912493107

Maarifi, G., Z. Hannoun, M.C. Geoffroy, F. El Asmi, K. Zarrouk, S. Nisole, D. Blondel, and M.K. Chelbi-Alix. 2016. MxA Mediates SUMO-Induced Resistance to Vesicular Stomatitis Virus. *J. Virol.* 90:6598–6610. https://doi.org/10.1128/JVI.00722-16

Manel, N., B. Hogstad, Y. Wang, D.E. Levy, D. Unutmaz, and D.R. Littman. 2010. A cryptic sensor for HIV-1 activates antiviral innate immunity in dendritic cells. *Nature.* 467:214–217. https://doi.org/10.1038/nature09337

Mowen, K.A., and M. David. 2014. Unconventional post-translational modifications in immunological signaling. *Nat. Immunol.* 15:512–520. https://doi.org/10.1038/ni.2873

Park, I.Y., R.T. Powell, D.N. Tripathi, R. Dere, T.H. Ho, T.L. Blasius, Y.C. Chiang, I.J. Davis, C.C. Fahey, K.E. Hacker, et al. 2016. Dual Chromatin and Cytoskeletal Remodeling by SETD2. *Cell.* 166:950–962. https://doi.org/10.1016/j.cell.2016.07.005

Png, C.W., and Y. Zhang. 2015. MAPK phosphatase 5 inhibits IRF3. *Oncotarget.* 6:19348–19349. https://doi.org/10.18632/oncotarget.5096

Polevoda, B., and F. Sherman. 2007. Methylation of proteins involved in translation. *Mol. Microbiol.* 65:590–606. https://doi.org/10.1111/j.1365-2958.2007.05831.x

Prinarakis, E., E. Chantzoura, D. Thanos, and G. Spyrou. 2008. S-glutathionylation of IRF3 regulates IRF3-CBP interaction and activation of the IFN beta pathway. *EMBO J.* 27:865–875. https://doi.org/10.1038/emboj.2008.28

Rahman, S., M.E. Sowa, M. Ottinger, J.A. Smith, Y. Shi, J.W. Harper, and P.M. Howley. 2011. The Brd4 extraterminal domain confers transcription activation independent of pTEFb by recruiting multiple proteins, including NSD3. *Mol. Cell. Biol.* 31:2641–2652. https://doi.org/10.1128/MCB.01341-10

Sabbattini, P., M. Sjoberg, S. Nikic, A. Frangini, P.H. Holmqvist, N. Kunowska, T. Carroll, E. Brookes, S.J. Arthur, A. Pombo, and N. Dillon. 2014. An H3K9/S10 methyl-phospho switch modulates Polycomb and Pol II binding at repressed genes during differentiation. *Mol. Biol. Cell.* 25:904–915. https://doi.org/10.1091/mbc.E13-10-0628

Sadler, A.J., and B.R. Williams. 2008. Interferon-inducible antiviral effectors. *Nat. Rev. Immunol.* 8:559–568. https://doi.org/10.1038/nri2314

Saitoh, T., A. Tun-Kyi, A. Ryo, M. Yamamoto, G. Finn, T. Fujita, S. Akira, N. Yamamoto, K.P. Lu, and S. Yamaoka. 2006. Negative regulation of interferon-regulatory factor 3-dependent innate antiviral response by the prolyl isomerase Pin1. *Nat. Immunol.* 7:598–605. https://doi.org/10.1038/ni1347

Suhara, W., M. Yoneyama, I. Kitabayashi, and T. Fujita. 2002. Direct involvement of CREB-binding protein/p300 in sequence-specific DNA binding of virus-activated interferon regulatory factor-3 holocomplex. *J. Biol. Chem.* 277:22304–22313. https://doi.org/10.1074/jbc.M200192200

Takeuchi, O., and S. Akira. 2009. Innate immunity to virus infection. *Immunol. Rev.* 227:75–86. https://doi.org/10.1111/j.1600-065X.2008.00737.x

Toyokawa, G., H.S. Cho, K. Masuda, Y. Yamane, M. Yoshimatsu, S. Hayami, M. Takawa, Y. Iwai, Y. Daigo, E. Tsuchiya, et al. 2011. Histone lysine methyltransferase Wolf-Hirschhorn syndrome candidate 1 is involved in human carcinogenesis through regulation of the Wnt pathway. *Neoplasia.* 13:887–898. https://doi.org/10.1593/neo.11048

Vougiouklakis, T., R. Hamamoto, Y. Nakamura, and V. Saloura. 2015. The NSD family of protein methyltransferases in human cancer. *Epigenomics.* 7:863–874. https://doi.org/10.2217/epi.15.32

Wang, C., X. Liu, Y. Liu, Q. Zhang, Z. Yao, B. Huang, P. Zhang, N. Li, and X. Cao. 2013. Zinc finger protein 64 promotes Toll-like receptor-triggered proinflammatory and type I interferon production in macrophages by enhancing p65 subunit activation. *J. Biol. Chem.* 288:24600–24608. https://doi.org/10.1074/jbc.M113.473397

Wang, G.G., L. Cai, M.P. Pasillas, and M.P. Kamps. 2007. NUP98-NSD1 links H3K36 methylation to Hox-A gene activation and leukaemogenesis. *Nat. Cell Biol.* 9:804–812. https://doi.org/10.1038/ncb1608

Yamagata, K., H. Daitoku, Y. Takahashi, K. Namiki, K. Hisatake, K. Kako, H. Mukai, Y. Kasuya, and A. Fukamizu. 2008. Arginine methylation of FOXO transcription factors inhibits their phosphorylation by Akt. *Mol. Cell.* 32:221–231. https://doi.org/10.1016/j.molcel.2008.09.013

Yang, P., L. Guo, Z.J. Duan, C.G. Tepper, L. Xue, X. Chen, H.J. Kung, A.C. Gao, J.X. Zou, and H.W. Chen. 2012. Histone methyltransferase NSD2/MMSET mediates constitutive NF-κB signaling for cancer cell proliferation, survival, and tumor growth via a feed-forward loop. *Mol. Cell. Biol.* 32:3121–3131. https://doi.org/10.1128/MCB.00204-12

Yoshioka, Y., T. Suzuki, Y. Matsuo, M. Nakakido, G. Tsurita, C. Simone, T. Watanabe, N. Dohmae, Y. Nakamura, and R. Hamamoto. 2016. SMYD3-mediated lysine methylation in the PH domain is critical for activation of AKT1. *Oncotarget.* 7:75023–75037.

Yu, Y., and G.S. Hayward. 2010. The ubiquitin E3 ligase RAUL negatively regulates type i interferon through ubiquitination of the transcription factors IRF7 and IRF3. *Immunity.* 33:863–877. https://doi.org/10.1016/j.immuni.2010.11.027

Zhang, M., Y. Tian, R.P. Wang, D. Gao, Y. Zhang, F.C. Diao, D.Y. Chen, Z.H. Zhai, and H.B. Shu. 2008. Negative feedback regulation of cellular antiviral signaling by RBCK1-mediated degradation of IRF3. *Cell Res.* 18:1096–1104. https://doi.org/10.1038/cr.2008.277

Zhang, Q., K. Zhao, Q. Shen, Y. Han, Y. Gu, X. Li, D. Zhao, Y. Liu, C. Wang, X. Zhang, et al. 2015. Tet2 is required to resolve inflammation by recruiting Hdac2 to specifically repress IL-6. *Nature.* 525:389–393. https://doi.org/10.1038/nature15252